

751 Appendix A Supplementary Methods

752 Total outflow length

753 To estimate Porphyron's total length from its projected length, we perform statistical deprojection.
 754 Equation 9 of Oei et al. [48] stipulates the probability density function (PDF) of an outflow's total length
 755 random variable (RV) L in case its projected length RV L_p is known to equal some value l_p . This PDF
 756 is parametrised by the tail index ξ of the Pareto distribution assumed to describe L . We calculate the
 757 median and expectation value of $L \mid L_p = l_p$ for tail indices $\xi = -3$ and $\xi = -4$, the integer values
 758 closest to the observationally favoured $\xi = -3.5 \pm 0.5$ [48].

759 First, we determine the cumulative distribution function (CDF) of $L \mid L_p = l_p$ through integration:

$$760 \quad F_{L|L_p=l_p}(l) := \int_{-\infty}^l f_{L|L_p=l_p}(l') \, dl' \quad (A1)$$

$$= \frac{-\xi}{2^{1+\xi}\pi} \frac{\Gamma^2\left(-\frac{\xi}{2}\right)}{\Gamma(-\xi)} \int_1^{\max\{x,1\}} \frac{x'^{\xi-1}}{\sqrt{x'^2-1}} \, dx',$$

760 where $x := \frac{l}{l_p}$ and $x' := \frac{l'}{l_p}$.

761 For $\xi = -3$, the CDF concretises to

$$762 \quad F_{L|L_p=l_p}(l) = \frac{3}{2} \int_1^{\max\{x,1\}} \frac{dx'}{x'^4 \sqrt{x'^2-1}} \quad (A2)$$

$$= \begin{cases} 0 & \text{if } x < 1; \\ \frac{(2x^2+1)\sqrt{x^2-1}}{2x^3} & \text{if } x \geq 1. \end{cases}$$

762 The median conditional total length, l_m , is defined by $F_{L|L_p=l_p}(l_m) := \frac{1}{2}$. Numerically, we obtain $x_m :=$
 763 $\frac{l_m}{l_p} \approx 1.0664$, or $l_m \approx 1.0664 l_p$. As $l_p = 6.43 \pm 0.05$ Mpc, we find $l_m = 6.86 \pm 0.05$ Mpc. An analogous
 764 numerical determination of the 16-th and 84-th percentiles then yields $l = 6.9^{+1.6}_{-0.4}$ Mpc.

765 For $\xi = -4$, the CDF concretises to

$$766 \quad F_{L|L_p=l_p}(l) = \frac{16}{3\pi} \int_1^{\max\{x,1\}} \frac{dx'}{x'^5 \sqrt{x'^2-1}} \quad (A3)$$

$$= \begin{cases} 0 & \text{if } x < 1; \\ \frac{2}{3\pi} \left(\frac{(3x^2+2)\sqrt{x^2-1}}{x^4} + 3 \arccos \frac{1}{x} \right) & \text{if } x \geq 1. \end{cases}$$

766 Numerically, we obtain $x_m \approx 1.0515$, or $l_m \approx 1.0515 l_p$, and thus $l_m = 6.76 \pm 0.05$ Mpc. In the same way
 767 as before, we find $l = 6.8^{+1.2}_{-0.3}$ Mpc.

768 Equation 10 of Oei et al. [48] gives a closed-form expression for $\mathbb{E}[L \mid L_p = l_p](\xi)$. Table 1 of the same
 769 work lists $\mathbb{E}[L \mid L_p = l_p](\xi = -3) = \frac{3\pi}{8}l_p$ and $\mathbb{E}[L \mid L_p = l_p](\xi = -4) = \frac{32}{9\pi}l_p$. In the case of Porphyron,
 770 these expressions concretise to $\mathbb{E}[L \mid L_p = l_p](\xi = -3) = 7.58 \pm 0.06$ Mpc and $\mathbb{E}[L \mid L_p = l_p](\xi = -4) =$
 771 7.28 ± 0.06 Mpc.

772 By conditioning L on more knowledge than a value for L_p alone, statistical deprojection could be made
 773 more precise. For example, one could additionally condition on the fact that Porphyron is generated
 774 by a Type 2 radiatively efficient (RE) AGN. If Type 1 RE AGN are seen mostly face-on and Type 2
 775 RE AGN are seen mostly edge-on, as proposed by the unification model [e.g. 27], then the detection of
 776 a Type 2 RE AGN would imply that the jets make a small angle with the sky plane. Extending the
 777 formulae to include this knowledge is beyond the scope of this work; however, mindful of the associated
 778 deprojection factor-reducing effect, we choose $\xi = -4$ as our fiducial tail index.

779 To assess Porphyron’s transport capabilities in a cosmological context, it is instructive to calculate
 780 its length relative to Cosmic Web length scales. In particular, the outflow’s total length relative to the
 781 typical cosmic void radius at its epoch is $f_v := l(1+z)R_v^{-1}$, where R_v is the typical comoving cosmic
 782 void radius. For $l = 6.8^{+1.2}_{-0.3}$ Mpc, $z = 0.896 \pm 0.001$, and $R_v = 20$ Mpc [13], we find $f_v = 64^{+12}_{-2}$ %. For
 783 our fiducial total length $l = 7$ Mpc, we find $f_v = 66\%$.

784 **Void penetration probability**

785 Porphyron’s orientation relative to its native Cosmic Web filament is currently unknown. We calculate
 786 the probability that an outflow breaches its filament, thus penetrating the surrounding voids, by assuming
 787 that jet orientations are independent from filament orientations. We furthermore assume that the jets
 788 are straight and of equal length, that the filament is of cylindrical shape, and that the host galaxy resides
 789 at the filament’s spine, where the gravitational potential is lowest. The RV Θ_f denotes the angle between
 790 the jet axis and the filament axis, whilst the constants R_f and $D_f := 2R_f$ denote the filament radius and
 791 diameter, respectively. An outflow of total length l penetrates voids with probability

$$\begin{aligned} \mathbb{P}(L \sin \Theta_f > D_f \mid L = l) &= \mathbb{P}\left(\sin \Theta_f > \frac{D_f}{l}\right) \\ &= 1 - F_{\sin \Theta_f}\left(\frac{D_f}{l}\right). \end{aligned} \quad (\text{A4})$$

792 The RV Θ_f has support on the interval $0 < \theta \leq \frac{\pi}{2}$. On this interval, the CDF is

$$\begin{aligned} F_{\Theta_f}(\theta) := \mathbb{P}(\Theta_f \leq \theta) &= \frac{1}{2\pi} \int_0^\theta \int_0^{2\pi} \sin \theta' \, d\varphi \, d\theta' \\ &= 1 - \cos \theta. \end{aligned} \quad (\text{A5})$$

793 The RV $\sin \Theta_f$ has support on the interval $0 < y \leq 1$. On this interval, the CDF is

$$\begin{aligned} F_{\sin \Theta_f}(y) &:= \mathbb{P}(\sin \Theta_f \leq y) = \mathbb{P}(\Theta_f \leq \arcsin y) \\ &= 1 - \cos \arcsin y = 1 - \sqrt{1 - y^2}, \end{aligned} \quad (\text{A6})$$

794 where we use the fact that the arcsine function is monotonically increasing. By combining Eqs. A4 and
795 A6, we obtain

$$\mathbb{P}(L \sin \Theta_f > D_f \mid L = l) = \begin{cases} 0 & \text{if } l \leq D_f; \\ \sqrt{1 - \left(\frac{D_f}{l}\right)^2} & \text{if } l > D_f. \end{cases} \quad (\text{A7})$$

796 Typically, however, we only know an outflow's *projected* length — not its *total* length. The quantity of
797 highest practical interest therefore is

$$\begin{aligned} p_v &:= \mathbb{P}(L \sin \Theta_f > D_f \mid L_p = l_p) \\ &= \mathbb{P}\left(L_p \frac{\sin \Theta_f}{\sin \Theta_o} > D_f \mid L_p = l_p\right) \\ &= \mathbb{P}\left(\frac{\sin \Theta_f}{\sin \Theta_o} > \frac{D_f}{l_p}\right) = 1 - F_X\left(\frac{D_f}{l_p}\right), \end{aligned} \quad (\text{A8})$$

798 where the RV Θ_o is the angle between the jet axis and the line of sight, and the RV X is the ratio of the RVs
799 $\sin \Theta_f$ and $\sin \Theta_o$. These latter RVs are independent and identically distributed: $F_{\sin \Theta_f}(y) = F_{\sin \Theta_o}(y)$.
800 We derive the PDF f_X by using the standard formula for the ratio distribution PDF (for independent
801 RVs). This formula demands the determination of $f_{\sin \Theta_f}(y) = f_{\sin \Theta_o}(y)$. From Eq. A6, we find that on
802 the interval $0 < y \leq 1$, the PDF is

$$f_{\sin \Theta_f}(y) = \frac{d}{dy} F_{\sin \Theta_f}(y) = \frac{y}{\sqrt{1 - y^2}}. \quad (\text{A9})$$

803 To find the distribution of X , it is helpful to distinguish three intervals. For $x \leq 0$, $f_X(x) = 0$, because
804 X is the ratio of two positive RVs. Then, for $0 < x < 1$,

$$f_X(x) = x \int_0^1 \frac{y^3}{\sqrt{1 - x^2 y^2} \sqrt{1 - y^2}} dy, \quad (\text{A10})$$

805 while for $x > 1$,

$$f_X(x) = x \int_0^{\frac{1}{x}} \frac{y^3}{\sqrt{1 - x^2 y^2} \sqrt{1 - y^2}} dy. \quad (\text{A11})$$

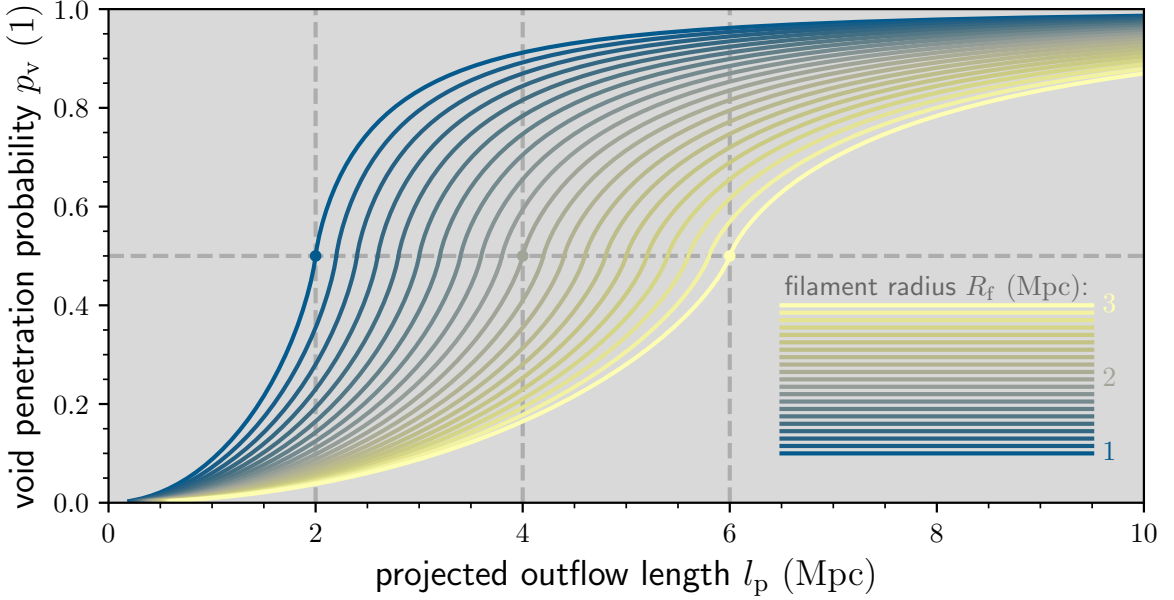


Fig. A1: From its projected length and an estimated radius for its native filament, one can calculate the probability that an outflow penetrates the surrounding voids. Outflows with projected lengths equaling the diameters of their filaments penetrate voids with 50% probability (as the dots exemplify).

806 Solving the integrals leads to

$$f_X(x) = \begin{cases} 0 & \text{if } x \leq 0; \\ \frac{(x^2+1) \ln \frac{1+x}{1-x} - 2x}{4x^2} & \text{if } 0 < x < 1; \\ \frac{(x^2+1) \ln \frac{x+1}{x-1} - 2x}{4x^2} & \text{if } x > 1. \end{cases} \quad (\text{A12})$$

807 At $x = 1$, f_X is undefined. We calculate F_X through integration, yielding

$$F_X(x) = \begin{cases} 0 & \text{if } x \leq 0; \\ \frac{1}{2} + \frac{1}{4} \left((x+1 - \frac{1}{x}) \ln \frac{1+x}{1-x} + \ln \frac{(1-x)^2}{1-x^2} \right) & \text{if } 0 < x < 1; \\ \frac{1}{2} + \frac{1}{4} \frac{x^2-1}{x} \ln \frac{x+1}{x-1} & \text{if } x > 1. \end{cases} \quad (\text{A13})$$

808 F_X is continuously extendable at $x = 1$ by defining $F_X(1) := \frac{1}{2}$. Finally, we define $x := \frac{D_f}{l_p}$, so that

809 $p_v(x) = 1 - F_X(x)$:

$$p_v(x) = \begin{cases} \frac{1}{2} - \frac{1}{4} \left((x+1 - \frac{1}{x}) \ln \frac{1+x}{1-x} + \ln \frac{(1-x)^2}{1-x^2} \right) & \text{if } 0 < x < 1; \\ \frac{1}{2} & \text{if } x = 1; \\ \frac{1}{2} - \frac{1}{4} \frac{x^2-1}{x} \ln \frac{x+1}{x-1} & \text{if } x > 1. \end{cases} \quad (\text{A14})$$

810 The median of X equals unity. Therefore, half of the outflows with projected lengths $l_p = D_f$ penetrate
 811 voids. For outflows with larger projected lengths, void penetration is more likely than not. Figure A1
 812 shows void penetration probabilities for physically relevant parameter ranges.

813 For Porphyron, we take l_p as before and adopt a filament (core) radius $R_f = 1.2$ Mpc [68]; this yields
 814 $x = 0.373 \pm 0.003$ and therefore $p_v = 95.2 \pm 0.1\%$.

815 **Filament shape modification**

816 We predict that powerful, long-lived outflows like Porphyron cause their host galaxies' filaments to
 817 expand thermally. Through lateral shocks, the jets distribute an amount of heat Q over the warm-hot
 818 IGM. This medium is sufficiently dilute that plasma interactions can be neglected; as a result, the ideal
 819 gas law, $pV = Nk_B T$, may be adopted as the equation of state. Here, p , V , N , and T are the filament's
 820 pressure, volume, plasma particle number, and temperature, respectively; k_B is Boltzmann's constant.
 821 Assuming a thermodynamic process at constant pressure and particle number, the work W is

$$W = p\Delta V = Nk_B\Delta T. \quad (\text{A15})$$

822 Before the outflow's emergence, the filament's equation of state is $pV_i = Nk_B T_i$, where V_i and T_i are
 823 its initial volume and temperature, respectively. Upon dividing Eq. A15 by this equation of state, one
 824 obtains

$$\frac{\Delta V}{V_i} = \frac{\Delta T}{T_i}. \quad (\text{A16})$$

825 Assuming that the filament retains a cylindrical shape, initially with radius r_i and finally with radius r_f ,
 826 and using that $\Delta V := V_f - V_i$, one obtains

$$\frac{r_f}{r_i} = \sqrt{1 + \frac{\Delta T}{T_i}}. \quad (\text{A17})$$

827 The radius ratio, $\frac{r_f}{r_i}$, depends only on the ratio between the temperature increase $\Delta T := T_f - T_i$ and the
 828 initial temperature. The temperature increase is

$$\Delta T = \frac{Q}{NC_{p,m}}, \quad (\text{A18})$$

829 where $C_{p,m}$ is the molar heat capacity at constant pressure. For a monatomic gas or a hydrogen plasma,
 830 $C_{p,m} = \frac{5}{2}R$, where R is the molar gas constant. The number of filamentary electrons and atomic nuclei

831 affected by the outflow is

$$N = \frac{\pi r_i^2 L \rho_i}{\mu m_p}, \quad (A19)$$

832 where L is the length of the cylindrical segment affected, ρ_i is the initial baryonic mass density, μ is
833 the average mass of a plasma particle relative to the proton mass, and m_p is the proton mass. We
834 estimate $\frac{L}{2}$ by multiplying the typical speed of lateral shocks with the outflow's lifetime. We decompose
835 $\rho_i = \rho_{c,0} \Omega_{\text{BM},0} (1+z)^3 (1+\delta)$, where z and δ are the filament's cosmological redshift and baryonic
836 overdensity, respectively.

837 We assess the outflow-induced morphological change to Porphyron's filament by evaluating Eq. A17,
838 taking $Q = 10^{55}$ J, $r_i = 1.2$ Mpc, $L = 7$ Mpc, $z = 0.9$, $1+\delta = 10$, $\mu = 0.5$, and $T_i = 10^7$ K; we find
839 $\Delta T = 9 \cdot 10^6$ K and $r_f = 1.7$ Mpc (an increase of $\sim 40\%$). Porphyron's heat dissipation renders the
840 outflow's native filament much hotter and thicker than it would have otherwise been.

841 ***Transport of heavy elements to voids***

842 Outflows from RE AGN could contain more heavy atoms than outflows from RI AGN: RE AGN tend
843 to reside in galaxies with higher star formation rates and thus more vigorous stellar winds, suggesting
844 increased entrainment of wind-borne atomic nuclei into jets [77]. The order-of-magnitude calculations
845 presented here, to be verified by future simulations, indicate that Mpc-scale outflows could supply Mpc³-
846 scale volumes in cosmic voids with significant heavy atoms, though consistent with upper limits [65].

847 We calculated the heavy element enrichment of the IGM in voids due to the deposition of atomic
848 nuclei initially entrained in the jets of Mpc-scale outflows. In particular, we estimated the final metallicity
849 in the deposition region considering both internal and external entrainment. Internal entrainment refers
850 to the entrainment into jets of atomic nuclei from stellar winds, *internal* to the host galaxy. External
851 entrainment refers to the entrainment into jets of atomic nuclei dwelling in the IGM, *external* to the
852 host galaxy.

853 Denoting the (two-sided) internal mass entrainment rate by \dot{M}_i , which we assumed constant through
854 time, the total internally entrained mass by an outflow of age T is

$$M_i = \dot{M}_i T. \quad (A20)$$

855 The internal mass entrainment rates of Centaurus A and 3C 31, both Fanaroff–Riley I (FR I) outflows
856 in the Local Universe, are estimated to be $\dot{M}_i = 2 \cdot 10^{-3} M_\odot \text{ yr}^{-1}$ [77] and $\dot{M}_i = 8 \cdot 10^{-3} M_\odot \text{ yr}^{-1}$
857 [35], respectively. At $M_\star = 6.3 \cdot 10^{11} M_\odot$, 3C 31's host stellar mass is similar to Porphyron's. However,
858 Porphyron is a Fanaroff–Riley II (FR II) outflow, suggesting a smaller jet opening angle ω and thus a

859 *smaller* \dot{M}_i . If ω is a factor of order unity smaller for FR II outflows than for FR I outflows [e.g. 36, 59],
 860 and $\dot{M}_i \propto \omega^2$, then $\dot{M}_{\text{FR II}} \sim 10^{-1} \dot{M}_{\text{FR I}}$. On the other hand, Porphyron’s host is seen much closer
 861 to the cosmic heyday of star formation, suggesting a larger SFR and thus a *larger* \dot{M}_i . After $z = 1.9$,
 862 SFRs S typically decayed exponentially with an e -folding time of 3.9 Gyr [e.g. 40]. If $\dot{M}_i \propto S$, then
 863 $\dot{M}_i(z = z_P) \sim e^2 \dot{M}_i(z = 0) \sim 10^1 \dot{M}_i(z = 0)$, where z_P is Porphyron’s redshift. Assuming that both
 864 effects are indeed of comparable importance, we provisionally adopted 3C 31’s $\dot{M}_i = 8 \cdot 10^{-3} M_\odot \text{ yr}^{-1}$
 865 as our fiducial value. Taking T as before, we obtained $M_i = 2 \cdot 10^7 M_\odot$. The total externally entrained
 866 mass is

$$M_e = 2 \int_0^{\frac{l}{2}} \rho_e(r) A_e(r) \, dr, \quad (\text{A21})$$

867 where $A_e(r)$ is the entrainment cross-section at a distance r from the AGN. Perhaps the simplest approach
 868 is to parametrise $A_e =: \pi R_e^2$, where R_e is a (constant) effective radius defined such that all baryons closer
 869 to the jet axis than R_e are entrained. Taking l and ρ_e as before, and $R_e = 1 \text{ kpc}$ [e.g. 55], we obtained
 870 $M_e = 4 \cdot 10^7 M_\odot$. Although highly uncertain, these estimates suggest that M_i and M_e can be of the same
 871 order of magnitude.

872 The total internally entrained mass in heavy elements is $Z_i M_i$, where Z_i is the mass-weighted mean
 873 metallicity of the galaxy’s stellar winds. The total externally entrained mass in heavy elements is $Z_e M_e$,
 874 where Z_e is the mass-weighted metallicity of the IGM along the jet. Assuming that the IGM in the voids
 875 is initially pristine, its final metallicity is

$$Z_v = \frac{Z_i M_i + Z_e M_e}{M_i + M_e + \rho_v V}, \quad (\text{A22})$$

876 where ρ_v is the baryon mass density within a deposition region of volume V . Taking a spherical deposition
 877 region with a diameter of 1 Mpc, and ρ_v as before, we obtained $\rho_v V = 7 \cdot 10^9 M_\odot$. Assuming $Z_i = Z_\odot$
 878 [e.g. 77] and $Z_e = 10^{-1} Z_\odot$ [e.g. 42], we found $Z_v = 3 \cdot 10^{-3} Z_\odot$. In conclusion, order-of-magnitude
 879 arguments suggest that void-penetrating Mpc-scale outflows can endow the local IGM with metallicities
 880 $Z_v \sim 10^{-3}\text{--}10^{-2} Z_\odot$.

881 *Quasar mass-based host galaxy candidate elimination*

882 SDSS J152933.03+601552.5 is the quasar-hosting galaxy 19'' north-northeast of J152932.16+601534.4,
 883 the galaxy we have identified as Porphyron’s host. We initially also considered SDSS
 884 J152933.03+601552.5 as a host galaxy candidate. However, aforementioned arguments involving the pres-
 885 ence of jets and their orientation and, to a lesser degree, arguments involving core radio luminosity and
 886 core synchrotron self-absorption all favour J152932.16+601534.4. We now discuss how our results would

887 change if, instead, SDSS J152933.03+601552.5 were Porphyron's host galaxy. Doing so will lead to a
 888 contradiction that disproves this alternative hypothesis.

889 First, we discuss results that do not require dynamical modelling. To start with, Porphyron would
 890 remain generated by an RE AGN. The host galaxy redshift would decrease from $z = 0.896 \pm 0.001$ to $z =$
 891 0.799 ± 0.001 , decreasing Porphyron's projected length from $l_p = 6.43 \pm 0.05$ Mpc to $l_p = 6.21 \pm 0.05$ Mpc.
 892 Again using $\xi = -4$, the total length would decrease from $l = 6.8_{-0.3}^{+1.2}$ Mpc to $l = 6.5_{-0.3}^{+1.2}$ Mpc and its
 893 conditional expectation from $\mathbb{E}[L \mid L_p = l_p] = 7.28 \pm 0.06$ Mpc to $\mathbb{E}[L \mid L_p = l_p] = 7.03 \pm 0.06$ Mpc. If
 894 orientation distinguishes Type 1 from Type 2 RE AGN, as the unification model supposes, then these
 895 statistical deprojection results may underestimate Porphyron's total length. Porphyron would remain
 896 the projectively largest galaxy-made structure identified so far. Porphyron's total radio luminosity at
 897 rest-frame wavelength $\lambda_r = 2$ m would decrease from $L_\nu = 2.8 \pm 0.3 \cdot 10^{26}$ W Hz $^{-1}$ to $L_\nu = 2.2 \pm 0.2 \cdot$
 898 10^{26} W Hz $^{-1}$.

899 Next, we discuss results that come from dynamical modelling. The jet power would decrease from $Q =$
 900 $1.3 \pm 0.1 \cdot 10^{39}$ W to $Q = 1.0 \pm 0.1 \cdot 10^{39}$ W, while the age would slightly increase from $T = 1.9_{-0.2}^{+0.7}$ Gyr to
 901 $T = 1.9_{-0.1}^{+0.7}$ Gyr.⁶ The transported energy would decrease from $E = 7.6_{-0.7}^{+2.1} \cdot 10^{55}$ J to $E = 6.4_{-0.6}^{+1.8} \cdot 10^{55}$ J,
 902 and the black hole mass gain from $\Delta M_\bullet > 8.5_{-0.8}^{+2.4} \cdot 10^8 M_\odot$ to $\Delta M_\bullet > 7.2_{-0.7}^{+2.0} \cdot 10^8 M_\odot$.

903 Finally, we arrive at a contradiction, as the quasar's SMBH mass (measured from its SDSS BOSS
 904 spectrum) $M_\bullet = 2.5 \pm 0.3 \cdot 10^8 M_\odot$ [11]. This mass is lower than the minimum mass gain associated to
 905 the fuelling of Porphyron's jets. Thus, assuming that SDSS J152933.03+601552.5 is the outflow's host
 906 galaxy leads to a contradiction. This argument reaffirms that J152932.16+601534.4 is Porphyron's host.

907 ***Diffusion of lobe plasma through voids***

908 When cosmic rays move through the jumbled magnetic fields of galaxy clusters and filaments of the
 909 Cosmic Web, the Lorentz force scatters them repeatedly. The mean free path of the ensuing random
 910 walk is so short that the CRs radiate away their energy before they are able to travel a cosmologically
 911 significant distance [e.g. 6]. Clusters and filaments thus effectively lock into place the CRs that are
 912 injected into them. By contrast, magnetic fields with Mpc-scale coherence lengths in voids are orders of
 913 magnitude weaker than those in clusters and filaments [e.g. 10], and as a result, CRs that are released
 914 into voids might diffuse through their entirety within a few gigayears. Void-filling diffusion of CRs might
 915 be especially rapid at early epochs: during Porphyron's lifetime, for instance, the proper volumes of
 916 voids were on average an order of magnitude smaller than they are today.

917 Consider a void region filled with relativistic particles, so that their velocity components obey

$$v_x^2 + v_y^2 + v_z^2 \approx c^2. \quad (\text{A23})$$

⁶Significant jet-mediated transport of heavy elements to the IGM would remain plausible. The host's stellar mass would decrease from $M_\star = 6.7 \pm 1.4 \cdot 10^{11} M_\odot$ to $M_\star = 4.0_{-0.3}^{+0.3} \cdot 10^{11} M_\odot$, while the SFR would become $S = 4.9_{-0.4}^{+0.3} \cdot 10^1 M_\odot \text{ yr}^{-1}$ [3].

918 We treat v_x , v_y , and v_z as random variables subject to the above constraint. If the particles have no bulk
 919 motion, and move in all directions with equal probability density,

$$\mathbb{E}[v_x^N] = \mathbb{E}[v_y^N] = \mathbb{E}[v_z^N] \quad (\text{A24})$$

920 for any $N \in \mathbb{R}$. In particular, given the absence of bulk motion, $\mathbb{E}[v_x] = \mathbb{E}[v_y] = \mathbb{E}[v_z] = 0$. By taking
 921 expectations on both sides of Eq. A23, using the linearity of expectation, and invoking Eq. A24, we find

$$\mathbb{E}[v_x^2] = \mathbb{E}[v_y^2] = \mathbb{E}[v_z^2] = \frac{c^2}{3}. \quad (\text{A25})$$

922 Without loss of generality, we assume the region's magnetic field \vec{B} to be oriented along the z -axis. The
 923 speed perpendicular to \vec{B} is $v_\perp = \sqrt{v_x^2 + v_y^2}$, so that, upon invoking Eq. A25, we find $\mathbb{E}[v_\perp^2] = \frac{2}{3}c^2$. A
 924 typical speed for relativistic particles perpendicular to a magnetic field thus is

$$\sqrt{\mathbb{E}[v_\perp^2]} = \sqrt{\frac{2}{3}}c \approx 0.8165 c. \quad (\text{A26})$$

925 Starting from Fick's first law of diffusion, and solving the case of Brownian motion in three dimensions,
 926 one obtains

$$r = \sqrt{6Dt}, \quad (\text{A27})$$

927 where r is the typical proper distance to the particles' origin after a time t . To find the diffusion coefficient
 928 D , we consider Bohm diffusion, in which charged particles diffuse through a turbulent magnetic field as
 929 a result of the Lorentz force. Whereas predicting the trajectory of any single charged particle requires
 930 knowledge of the specific magnetic field structure in its surroundings, the statistical properties of Bohm
 931 diffusion are determined solely by the statistical properties of the magnetic field and the charge and
 932 energy of the diffusing particles. The Larmor radius for a particle with Lorentz factor γ , total velocity
 933 v , rest mass m , and charge q , is

$$r_L = \frac{\gamma(v)mv_\perp}{|q|B}. \quad (\text{A28})$$

934 For a relativistic particle whose v_\perp is given by Eq. A26, we obtain a Larmor radius

$$r_L(E) = \sqrt{\frac{2}{3}} \frac{E}{c|q|B} = 8.8 \cdot 10^2 \text{ pc} \cdot \frac{E}{1 \text{ GeV}} \cdot \frac{10^{-15} \text{ G}}{B}, \quad (\text{A29})$$

935 where E is the total (i.e. rest plus kinetic) energy of the particle. The diffusion coefficient for charged
 936 particles in a magnetic field with a Kolmogorov turbulence spectrum is well approximated [21] by

$$D(E) \approx D_{\text{Bohm}}(E_0) \left(\frac{E}{E_0} \right)^{\frac{1}{3}} + D_{\text{Bohm}}(E_1) \left(\frac{E}{E_1} \right)^2. \quad (\text{A30})$$

937 Here, E_0 is the energy for which the circumference of gyration equals the magnetic field coherence length
 938 λ_c :

$$2\pi r_L(E_0) = \lambda_c. \quad (\text{A31})$$

939 For $q = \pm e$, where e is the elementary charge, this equation implies that

$$E_0 = \sqrt{\frac{3}{2}} \frac{\lambda_c c |q| B}{2\pi} = 1.8 \cdot 10^2 \text{ GeV} \cdot \frac{\lambda_c}{1 \text{ Mpc}} \cdot \frac{B}{10^{-15} \text{ G}}. \quad (\text{A32})$$

940 Furthermore, $E_1 = \frac{3}{2}E_0$. The Bohm diffusion coefficient [e.g. 21] D_{Bohm} is

$$D_{\text{Bohm}}(E) = \frac{c}{3} r_L(E) \quad (\text{A33})$$

$$= 9.0 \cdot 10^{-2} \frac{\text{Mpc}^2}{\text{Gyr}} \cdot \frac{E}{1 \text{ GeV}} \cdot \frac{10^{-15} \text{ G}}{B}. \quad (\text{A34})$$

941 We note that

$$D_{\text{Bohm}}(E_0) = \frac{c}{6\pi} \lambda_c = 1.6 \cdot 10^1 \frac{\text{Mpc}^2}{\text{Gyr}} \cdot \frac{\lambda_c}{1 \text{ Mpc}} \quad (\text{A35})$$

942 is independent of the void's magnetic field strength. Because $D_{\text{Bohm}} \propto r_L \propto E$, we have $D_{\text{Bohm}}(E_1) =$
 943 $\frac{3}{2}D_{\text{Bohm}}(E_0)$.

944 For $E = 1 \text{ GeV}$, $\lambda_c = 1 \text{ Mpc}$, and $B = 10^{-15} \text{ G}$, we find $D(E) = 2.9 \frac{\text{Mpc}^2}{\text{Gyr}}$. After $t = 1 \text{ Gyr}$, the
 945 typical displacement of cosmic rays that escaped from the outflow's lobes is $r = 4.2 \text{ Mpc}$. We note that r
 946 scales slowly with particle energy, magnetic field strength, and (to a lesser degree) with coherence length:

$$r \propto E^{\frac{1}{6}} B^{-\frac{1}{6}} \lambda_c^{\frac{1}{3}} t^{\frac{1}{2}}. \quad (\text{A36})$$

947 For short time intervals t , we can ignore the expansion of the Universe; defining $r_c := r(1 + z)$, the void
 948 volume-filling fraction \mathcal{V} of a single lobe becomes

$$\mathcal{V} = \left(\frac{2r_c}{D_c} \right)^3. \quad (\text{A37})$$

949 For sufficiently short time intervals t , particles move in rectilinear fashion, and the typical proper
 950 displacement of a relativistic particle within t is $r = ct$, not $r = \sqrt{6Dt}$. Diffusion can only possibly provide
 951 an accurate description of the typical displacement for sufficiently large t . As superluminal motion is
 952 impossible,

$$\sqrt{6Dt} < ct, \text{ or } t > \frac{6D}{c^2} =: \tau_d, \quad (\text{A38})$$

953 where τ_d is the diffusion timescale (as in Globus et al. [21], but with a factor 6 instead of 4). Diffusion
 954 only has a role to play in the description of particle movement through voids when $\tau_d < \tau_b$, the ballistic
 955 timescale for particle movement through voids. We define

$$\tau_b := \frac{R_c}{(1 + z)c}, \quad (\text{A39})$$

956 where R_c is the comoving void radius. As $\tau_d \propto D$, there is a maximum diffusion coefficient, D_{\max} , above
 957 which the diffusive description is invalid. Solving $\tau_d(D_{\max}) = \tau_b$ for D_{\max} , we obtain

$$D_{\max} = \frac{R_c c}{6(1 + z)}. \quad (\text{A40})$$

958 This maximum diffusion coefficient corresponds to a minimum magnetic field strength, B_{\min} . Approximating
 959 $D_{\max} \approx D_{\text{Bohm}}(E, B_{\min})$, we find

$$B_{\min} = 2\sqrt{\frac{2}{3}} \frac{(1 + z)E}{c|q|R_c} \quad (\text{A41})$$

$$= 8.8 \cdot 10^{-20} \text{ G} \cdot \frac{E}{1 \text{ GeV}} \cdot \frac{20 \text{ Mpc}}{R_c} \cdot \frac{1 + z}{1} \cdot \frac{e}{|q|}. \quad (\text{A42})$$

960 We should only apply diffusion theory to the problem of particle movement through voids for void
 961 magnetic field strengths $B \gg B_{\min}$. For particle energies of 1 GeV, we therefore only consider diffusion
 962 for $B \gtrsim 10^{-18}$ G.

963 The diffusing cosmic rays lose energy over time. In voids, losses by inverse Compton scattering to
 964 CMB photons are by far more important than losses by synchrotron radiation, because

$$\frac{P_{\text{IC,CMB}}}{P_s} = \frac{B_{\text{CMB}}^2(z)}{B^2}, \quad (\text{A43})$$

965 and $B_{\text{CMB}}^2(z) \gg B^2$ in voids. (Here, P_{IC} and P_s are, respectively, the inverse Compton and synchrotron
 966 powers of a single cosmic ray.) The inverse Compton loss timescale for an electron or positron of total
 967 energy E at cosmological redshift z is

$$\tau_{\text{IC,CMB}}(E, z) := \frac{E}{P_{\text{IC,CMB}}(E, z)} \quad (\text{A44})$$

$$= \frac{6m_e^2 c^3 \mu_0}{4\beta^2 E \sigma_T B_{\text{CMB}}^2(0)(1+z)^4} \quad (\text{A45})$$

$$= 1.2 \text{ Gyr} \cdot \frac{1}{\beta^2} \cdot \frac{1 \text{ GeV}}{E} \cdot \frac{1}{(1+z)^4}, \quad (\text{A46})$$

968 where σ_T is the Thomson cross-section for electrons and positrons. For protons, the inverse Compton loss
 969 timescale equals the above multiplied by a factor $\left(\frac{m_p}{m_e}\right)^4 \approx 1.1 \cdot 10^{13}$. Therefore, for non-ultra-high-energy
 970 cosmic ray protons, both synchrotron *and* inverse Compton losses are negligible.

971 Because $\frac{dD}{dE} > 0$, diffusion slows down as particles lose energy; in other words, a particle's *highest*
 972 diffusion coefficient is its *initial* diffusion coefficient.

973 Let X_c be the comoving displacement along the x -direction. We consider N time steps, each of length
 974 $\tau := \frac{t}{N}$. Let $X_{c,i}$ be the comoving displacement along the x -direction achieved in the i -th time step, and
 975 let X_i be the corresponding proper displacement.

$$X_c := \sum_{i=1}^N X_{c,i} \quad (\text{A47})$$

976 Because $\mathbb{E}[X_{c,i}] = 0$, $\mathbb{E}[X_c] = \sum_{i=1}^N \mathbb{E}[X_{c,i}] = 0$. Therefore

$$\mathbb{E}[X_c^2] = \mathbb{V}[X_c] = \sum_{i=1}^N \mathbb{V}[X_{c,i}] = \sum_{i=1}^N \mathbb{E}[X_{c,i}^2]. \quad (\text{A48})$$

977 Because $X_{c,i} = (1+z_i)X_i$, $\mathbb{E}[X_{c,i}^2] = (1+z_i)^2 \mathbb{E}[X_i^2]$. Therefore

$$\mathbb{E}[X_c^2] = \sum_{i=1}^N (1+z_i)^2 \frac{\mathbb{E}[X_i^2]}{2\tau} \cdot 2\tau. \quad (\text{A49})$$

978 Following Einstein's definition of the diffusion coefficient, the proper diffusion coefficient in the x -direction
 979 for the i -th time step, $D_{x,i}$, is

$$D_{x,i} := \frac{\mathbb{E}[X_i^2]}{2\tau}. \quad (\text{A50})$$

980 We can then write

$$\mathbb{E}[X_c^2] = 2\tau \sum_{i=1}^N (1+z_i)^2 D_{x,i}. \quad (\text{A51})$$

981 Proceeding analogously for the y - and z -directions, and defining $R_c^2 := X_c^2 + Y_c^2 + Z_c^2$, we find

$$\mathbb{E}[R_c^2] = \mathbb{E}[X_c^2] + \mathbb{E}[Y_c^2] + \mathbb{E}[Z_c^2] \quad (\text{A52})$$

$$= 2\tau \sum_{i=1}^N (1+z_i)^2 (D_{x,i} + D_{y,i} + D_{z,i}). \quad (\text{A53})$$

982 In the isotropic case, $D_{x,i} = D_{y,i} = D_{z,i} =: D_i$, so that

$$\mathbb{E}[R_c^2] = 6\tau \sum_{i=1}^N (1+z_i)^2 D_i = 6t \cdot \frac{1}{N} \sum_{i=1}^N (1+z_i)^2 D_i. \quad (\text{A54})$$

983 Denoting the (time) average of a function $f(t)$ by $\langle f \rangle$, we have

$$r_c := \sqrt{\mathbb{E}[R_c^2]} = \sqrt{6\langle(1+z)^2 D\rangle t}. \quad (\text{A55})$$

984 Let E be an RV denoting particle energy, and let f_E be its PDF. Let n_l be the lobe particle number
 985 density, and let R_l be the lobe radius. The number of particles in an outer shell with thickness ΔR with
 986 energies between E and $E + dE$ is

$$dN(E) = 4\pi R_l^2 \Delta R \cdot n_l f_E(E) dE. \quad (\text{A56})$$

987 These particles escape from the shell over a timescale

$$\tau_e(E) = \frac{\Delta R^2}{2D_{\perp,c}(E)}, \quad (\text{A57})$$

988 where $D_{\perp,c}$ is the compound cross-field diffusion coefficient [19]. The number of particles with energies
 989 between E and $E + dE$ escaping from the shell per unit of time thus is

$$\frac{dN(E)}{\tau_e(E)} = \frac{8\pi R_1^2 \cdot D_{\perp,c}(E) \cdot n_l f_E(E) dE}{\Delta R}. \quad (\text{A58})$$

990 The particulate energy escaping from the shell per unit of time and unit of energy, which we shall call
 991 the power density P_E , is

$$P_E(E) := E \cdot \frac{dN(E)}{\tau_e(E) dE} = \frac{8\pi R_1^2 \cdot D_{\perp,c}(E) \cdot n_l f_E(E) E}{\Delta R}. \quad (\text{A59})$$

992 Finally, the total power P is

$$P := \int_E P_E(E) dE = \frac{8\pi R_1^2 n_l}{\Delta R} \int_E D_{\perp,c}(E) E f_E(E) dE \quad (\text{A60})$$

$$= \frac{8\pi R_1^2 n_l}{\Delta R} \mathbb{E}_E[D_{\perp,c}(E) E]. \quad (\text{A61})$$

993 The compound cross-field diffusion coefficient is [17]

$$D_{\perp,c}(E) \approx D_{\perp}(E) \left(1 + \frac{\Lambda^2(E)}{\ln \Lambda(E)} \right), \quad (\text{A62})$$

994 where D_{\perp} is the cross-field diffusion coefficient, given by

$$D_{\perp}(E) \approx \frac{c}{3} r_L(E) \delta_B(r_L(E)). \quad (\text{A63})$$

995 Here

$$\delta_B(l) \approx f_i \cdot \left(\frac{l}{l_i} \right)^{\frac{2}{3}}, \quad (\text{A64})$$

996 where l_i is the turbulence injection scale and f_i is the total turbulence energy density up to this scale,
 997 relative to the energy density of the thermal medium surrounding the lobe [19]. Additionally,

$$\Lambda(E) = \frac{1}{\sqrt{2}} \frac{\delta_B(\lambda_{c,l})}{\delta_B(r_L(E))} = \frac{1}{\sqrt{2}} \left(\frac{\lambda_{c,l}}{r_L(E)} \right)^{\frac{2}{3}}, \quad (\text{A65})$$

998 where $\lambda_{c,1}$ is the lobe's magnetic field correlation length. We assume that E has a Pareto distribution
 999 [e.g. 73], so that its PDF, f_E , (for $p \neq -1$) is given by

$$f_E(E) = \begin{cases} \frac{p+1}{E_{\max}^{p+1} - E_{\min}^{p+1}} E^p & \text{if } E_{\min} < E < E_{\max}; \\ 0 & \text{otherwise;} \end{cases} \quad (\text{A66})$$

1000 and $E_{\min} := \gamma_{\min} mc^2$ and $E_{\max} := \gamma_{\max} mc^2$. We calculated the total power assuming $R_l = 100$ kpc,
 1001 $\Delta R = \lambda_{c,1} = 10$ kpc, $l_i = 10$ kpc, $f_i = 10^{-2}$, $B = B_l = 10^{-7}$ G, $|q| = e$, $m = m_e$, $p = -2.4$, $\gamma_{\min} = 10$,
 1002 $\gamma_{\max} = 10^5$, and $n_l = 10^{-10}$ cm $^{-3}$. We find $P = 10^{30}$ W.

1003 To estimate the final void magnetic field strength B_v , we followed an argument akin to that in Beck
 1004 et al. [4]. If the lobe would expand to fill the entire void, then magnetic flux conservation yields

$$B_v = B_l \left(\frac{R_l}{R_v} \right)^2. \quad (\text{A67})$$

1005 By squaring and dividing both sides of this equation by $2\mu_0$, one recasts it in terms of magnetic energy
 1006 densities and obtains

$$u_{B_v} = u_{B_l} \left(\frac{R_l}{R_v} \right)^4. \quad (\text{A68})$$

1007 However, only a fraction of the lobe's magnetic energy can escape, and it is only this fraction that we
 1008 should consider in our calculation. If we assume that the magnetic energy that is carried out of the lobe
 1009 is comparable to the energy of the escaped particles, which equals Pt , then

$$u_{B_v} = \frac{Pt}{E_l} u_{B_l} \left(\frac{R_l}{R_v} \right)^4, \quad (\text{A69})$$

1010 where E_l is the total magnetic energy of the lobe. Recasting this equation back to magnetic field strengths,
 1011 we obtain

$$B_v = \sqrt{\frac{Pt}{E_l}} \left(\frac{R_l}{R_v} \right)^2 B_l. \quad (\text{A70})$$

1012 The energy ratio in Beck et al. [4]'s analogous Eq. 4 should likewise appear under a square root. This
 1013 is a matter of typography only: the authors did take the square root to obtain their results (private
 1014 communication with M. Hanasz). For $t = 10^0$ Gyr, $E_l = 10^{55}$ J, $R_v = 10^1$ Mpc, and P , R_l , and B_l as
 1015 before, we obtained $B_v = 6 \cdot 10^{-16}$ G.